The Journal of Chemical Physics

Predicting water's phase diagram and liquid-state anomalies

Thomas M. Truskett and Ken A. Dill

Citation: J. Chem. Phys. **117**, 5101 (2002); doi: 10.1063/1.1505438
View online: http://dx.doi.org/10.1063/1.1505438
View Table of Contents: http://jcp.aip.org/resource/1/JCPSA6/v117/i11
Published by the American Institute of Physics.

Additional information on J. Chem. Phys.

Journal Homepage: http://jcp.aip.org/
Journal Information: http://jcp.aip.org/about/about_the_journal
Top downloads: http://jcp.aip.org/features/most_downloaded
Information for Authors: http://jcp.aip.org/authors

ADVERTISEMENT

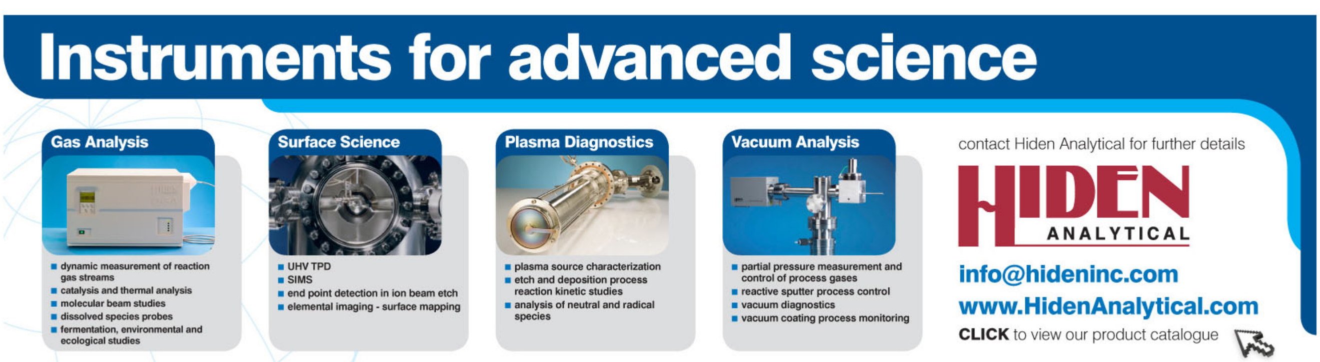

Downloaded 15 Mar 2013 to 146.201.208.22. Redistribution subject to AIP license or copyright; see http://jcp.aip.org/about/rights_and_permissions

JOURNAL OF CHEMICAL PHYSICS VOLUME 117, NUMBER 11 15 SEPTEMBER 2002

COMMUNICATIONS

Predicting water's phase diagram and liquid-state anomalies

Thomas M. Truskett[a)] and Ken A. Dill
Department of Pharmaceutical Chemistry, University of California, San Francisco, San Francisco, California 94143-1204

(Received 10 May 2002; accepted 16 July 2002)

Water expands upon freezing, has minima in its volume, heat capacity, and isothermal compressibility with temperature, and shows signs of a first-order phase transition when supercooled. We present an analytical molecular theory that can account for these behaviors. It suggests that local network formation and hydrogen-bonding cooperativity between triplets of neighboring molecules are keys to understanding water's thermodynamics. © *2002 American Institute of Physics.* [DOI: 10.1063/1.1505438]

INTRODUCTION

Simple analytical models—the ideal gas, the van der Waals (vdW) fluid, the Einstein crystal—have considerably advanced our understanding of materials. The role of analytical models is different from, and complementary to, that of detailed molecular simulations. Simulations are virtual experiments. However, they are limited, even with the fastest computers, to exploring relatively short time and length scales. Analytical models are typically simpler and more approximate, but they can give direct insights into how material properties arise from microscopic interactions. Moreover, analytical models can often treat a broad range of conditions, reveal trends and universal principles (e.g., the law of corresponding states), suggest functional relations for engineering applications, and motivate experiments. In this Communication, we develop an analytical model for water.

One of the most basic theories for simple molecular and colloidal fluids is the vdW model. It shows how such systems can be qualitatively understood by considering two competing tendencies. Intermolecular attractions favor condensed states at low temperatures (where energy dominates), while expanded vapor states prevail at high temperatures (where entropy dominates). However, this description is not adequate for water.[1] Water molecules form hydrogen bonds (h-bonds) that are both directional and "cooperative;"[2–5] i.e., the strength of an h-bond depends on the bonding states of neighboring molecules. For example, when an h-bond forms between two water molecules, their charge distributions change so as to strengthen an h-bond with a third water. Water's h-bonding results in chains and open networks—structural features that are thought to be principal components of its anomalous behavior,[6–8] including the liquid's distinctive minima in volume, isothermal compressibility, and isobaric heat capacity at 4, 46.5 and 36 °C, respectively.

Recent theoretical treatments[9,10] have extended the vdW model to incorporate hydrogen-bonding interactions. These models are able to reproduce many of liquid water's distinctive properties. However they do not account for water's solid "ice" phases, and they are not designed to predict the h-bond structures present in the liquid phase. Here we develop a statistical mechanical model that gives simple insights into water's h-bond structures, its thermodynamic anomalies, and its phase diagram. The model incorporates, at the level of triplets of neighboring molecules, two key effects of h-bonding in water: (1) the energetic preference for open h-bond structures and (2) the cooperativity of h-bond interactions.

THE MODEL

Our model bears structural resemblance to the Mercedes Benz (MB) model,[11] which shows[12] many of water's peculiar physical properties. However, the energetics of the two models are somewhat different. We consider N water molecules, each of which is modeled as a two-dimensional (2D) disk of diameter d. Each water has three identical bonding arms arranged as in the MB logo (see Fig. 1). We focus on triplets of molecules (labeled A, B, and C in Fig. 1). In the vapor and liquid phases, each triplet can fluctuate between three states. The lowest energy state represents the cooperative *cagelike* structures found in ice.[12] This state has energy $u_1(\phi) = -\epsilon_{HB} + k_S\phi^2$, where $-\epsilon_{HB}$ is an h-bond energy constant, k_S is the vibrational spring constant of the h-bond, and ϕ is the angle shown in Fig. 1. This term implies h-bond cooperativity because the strength of the interaction between molecules B and C depends on the bonding angle with A. The 2D "volume"[13] of the perfectly bonded cagelike state is $v_1 = 3\sqrt{3}d^2/4$. The next higher energy level is a *dense* state with three vdW contacts, where B's h-bonds with A and C are broken. Its energy is $u_2 = -\epsilon_d$, where ϵ_d is a constant, and its local volume is $v_2 = (2+\sqrt{3})d^2/4$. The highest energy level is an *expanded* state with neither h-bonds nor vdW contacts. Its energy is $u_3 = 0$ and its local volume is assumed[14] to be that of an excluded-volume gas $v_3 = (\beta P)^{-1} + v_2$, where $\beta = (k_B T)^{-1}$, k_B is Boltzmann's constant, T is temperature, and P is pressure. To account for

[a)]Permanent address: Department of Chemical Engineering, The University of Texas at Austin, Austin, Texas 78712-1062.

 © 2002 American Institute of Physics

Downloaded 15 Mar 2013 to 146.201.208.22. Redistribution subject to AIP license or copyright; see http://jcp.aip.org/about/rights_and_permissions

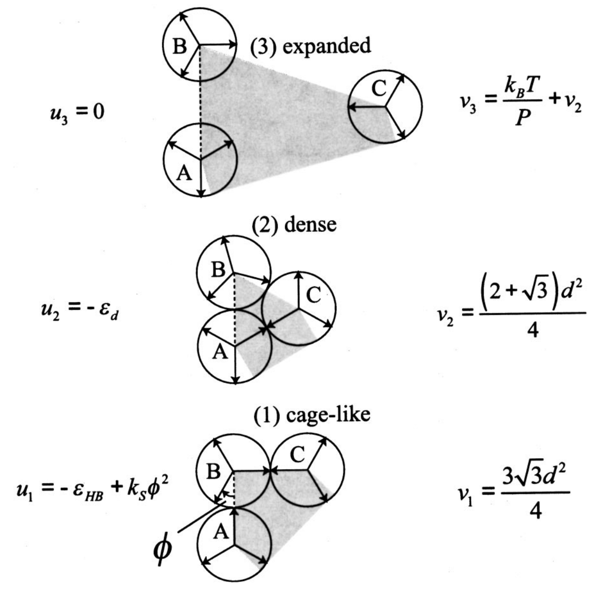

FIG. 1. Molecular triplets (in order of increasing energy): (1) *cagelike*, (2) *dense*, and (3) *expanded*. Volumes v_j ($j=1,2,3$) are computed using house-shaped cells (Ref. 14) (shaded) that contain sectors of molecules A, B, and C. The sectors sum to $\pi d^2/4$; i.e., one total molecule per cell. As in traditional cell theories (Ref. 16), we account for the degrees of freedom of central molecule B as it moves within the constraints of its cell. In the cagelike state, B remains in contact with A and C. B maintains a perfect h-bond with C, but the A–B bond bends as B rotates. In the dense state, A, B, and C are in mutual contact, and B's orientation is not constrained by bonds. The expanded state has neither h-bonds nor vdW contacts. B's orientation ϕ is measured with respect to the axis connecting the centers of A and B.

interactions beyond the triplet level, we include a global attractive energy $-Na/v$, where a is the vdW dispersion parameter and v is the average molar volume.[14,15]

The isothermal–isobaric (constant N, T, and P) partition function for molecule B can be expressed as[14]

$$\Delta_{\text{cell}} = c(\beta) N \sum_{j=1}^{3} \int\int dx\, dy \int d\phi \exp(-\beta[u_j + P v_j]), \quad (1)$$

where the sum is over the three possible states of the triplet *cell* (see Fig. 1), x and y are the coordinates of molecule B, and $c(\beta)$ results from integrating over the momenta. The factor N in Eq. (1) accounts for the fact that each of the N molecules can be the central molecule (B) of a cell. The partition function for the system of N molecules Δ is obtained by substituting Eq. (1) into $\Delta = \Delta_{\text{cell}}^N / N!$, integrating over the allowed values of x, y, and ϕ, and applying Stirling's approximation $N! \simeq (N/e)^N$, to get

$$\Delta = \left(\sum_{j=1}^{3} \Delta_j \right)^N. \quad (2)$$

Here $\Delta_j = g_j \exp[-\beta(\langle u_j \rangle + P v_j)]$, where $\langle u_j \rangle$ is the average energy of triplet state j,

$$\langle u_1 \rangle = -\epsilon_{HB} + \frac{1}{2\beta} - \frac{\sqrt{k_S \pi/\beta}\, \exp(-\beta k_S \pi^2/9)}{3\, \text{erf}(\sqrt{\beta k_S \pi^2/9})},$$
$$\langle u_2 \rangle = -\epsilon_d, \quad (3)$$
$$\langle u_3 \rangle = 0,$$

and the g_j's are densities of states.

$$g_1 = 2\pi d^2 c(\beta) e \frac{\text{erf}(\sqrt{\beta k_S \pi^2/9})}{\sqrt{\beta k_S \pi}} \times \exp\left(\frac{1}{2} - \frac{\sqrt{\beta k_S \pi}\, \exp(-\beta k_S \pi^2/9)}{3\, \text{erf}(\sqrt{\beta k_S \pi^2/9})} \right),$$
$$g_2 = 2\pi d^2 c(\beta) e, \quad (4)$$
$$g_3 = \frac{2\pi c(\beta) e}{\beta P}.$$

A derivation and a discussion of the approximations associated with Eqs. (1)–(4) are given in Ref. 14.

This model provides a highly simplified picture of water's hydrogen bonds, vdW attractions, and steric repulsions. Its main limitations are (1) the 2D geometry of the model does not accurately reflect water's molecular details and (2) the partition function does not account for correlations between neighboring triplet cells—an approximation that may not be accurate at low temperatures. The model's strengths include its simple analytical form and its ability to provide insights into a broad range of experimentally observed thermodynamic and structural properties of pure water.

THERMODYNAMIC ANOMALIES

The liquid and vapor properties of the model can be computed from Δ using standard thermodynamic relationships. For example, the chemical potential is given by $\mu(\beta,P) = -(\beta N)^{-1} \ln \Delta$ and the molar volume (i.e., the equation of state) is given by $v(\beta,P) = (\partial \mu / \partial P)_\beta$.[16,17] In contrast to molecular simulations using microscopically detailed potentials, thermodynamic properties of the present model can be calculated in a few seconds on a personal computer.

Figure 2 compares the predicted and experimental[18] behavior of the reduced volume v_r, thermal expansion coefficient α_P^*, isothermal compressibility κ_T^*, and heat capacity c_P. The theory captures water's distinctive anomalies: minimum in v_r, expansion upon cooling ($\alpha_P^* < 0$), and minima in both κ_T^* and c_P.

HYDROGEN-BOND STRUCTURES

To understand the structural basis for these thermodynamic properties, we studied the populations $f_j = \Delta_j / (\sum_{k=1}^{3} \Delta_k)$ of the three different states that triplets of neighboring molecules can exhibit [see Fig. 3(a)]. The populations show that the molecules in the supercooled liquid are in predominantly h-bonded, cagelike configurations. As the liquid is heated, h-bonds break and the cagelike structures collapse into denser states of higher enthalpy. This collapse underlies the supercooled liquid's negative thermal expansion coefficient ($\alpha_P^* < 0$) and its large heat capacity. Applying pressure to the supercooled liquid shifts the cell population from open cagelike to dense structures. This explains the large isothermal compressibility in supercooled water. Heating warm water breaks the vdW contacts of the dense states,

Downloaded 15 Mar 2013 to 146.201.208.22. Redistribution subject to AIP license or copyright; see http://jcp.aip.org/about/rights_and_permissions

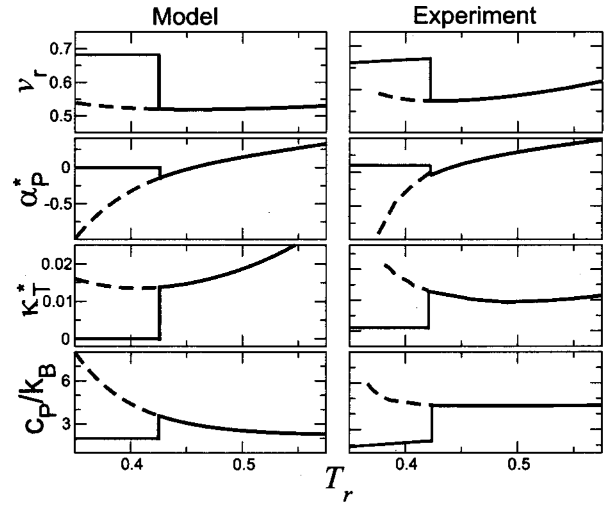

FIG. 2. Properties of the liquid at atmospheric pressure: (left) model and (right) experiments (Ref. 18). Unbroken curves represent the stable liquid and crystalline phases, and dashed curves represent the supercooled liquid. Discontinuities occur at the freezing point. The properties are volume v_r, thermal expansion coefficient α^*_P, isothermal compressibility κ^*_T, and isobaric heat capacity c_P/k_B. Comparison with experiments requires reduced variables: $T_r = T/T_C$, $P_r = P/P_C$, $v_r = v/v_C$, $\kappa^*_T = -(\partial \ln v_r/\partial P_r)_{T_r}$, and $\alpha^*_P = (\partial \ln v_r/\partial T_r)_{P_r}$. Subscript C denotes the value at the liquid–vapor critical point. In this representation, the predictions depend on three parameters, which we choose to be $a/(\epsilon_{HB} d^2) = 0.295$, $\epsilon_d/\epsilon_{HB} = 0.15$, and $k_S/\epsilon_{HB} = 10^5$. The model's "atmospheric" pressure is $P_r = 0.1627$, where it exhibits freezing and boiling temperatures of $T_r = 0.4255$ and $T_r = 0.5804$ (see Fig. 4), approximating water's normal freezing and boiling temperatures of $T_r = 0.422$ and 0.577, respectively.

causing it to have positive thermal expansivity ($\alpha^*_P > 0$). The theory correctly predicts that water's anomalies shown in Fig. 2 are suppressed at high pressure,[14] a result that is readily interpreted by Le Chatelier's principle: Compression shifts the equilibrium liquid structure away from the high-volume cagelike structures (characteristic of water) to the low-volume dense structures (characteristic of simpler liquids).

The populations shown in Fig. 3(a) are qualitatively similar to water's h-bond populations as deduced from IR spectroscopic data.[3] Based on an analysis of OH stretching bands, Luck[3] has identified three distinct types of OH states in the liquid (listed in order of increasing energy): strongly cooperative h-bonded, weakly cooperative h-bonded, and nonbonded. These states are analogous to our model's cage-like, dense, and expanded energy levels, respectively. Figure 3(b) shows the effect of temperature on water's h-bond populations. Strongly cooperative h-bonds are prevalent in cold water. Heating melts the strongly cooperative structures into weakly cooperative and nonbonded states at intermediate temperatures. Finally, the weakly cooperative h-bonds break to form nonbonded states as the liquid approaches the critical point. A comparison of Figs. 3(a) and 3(b) shows that the present model captures these experimental observations.

The results of Fig. 3(a) are also consistent with the *ab initio* molecular cluster populations predicted by Weinhold's quantum cluster equilibrium (QCE) theory[4] for water.[5] In zeroth-order QCE theory, strongly cooperative cyclic clusters prevail at low temperatures, smaller and less cooperative structures emerge at intermediate temperatures, and non-bonded monomers dominate at high temperatures (see, e.g., Fig. 3 in Ref. 5).

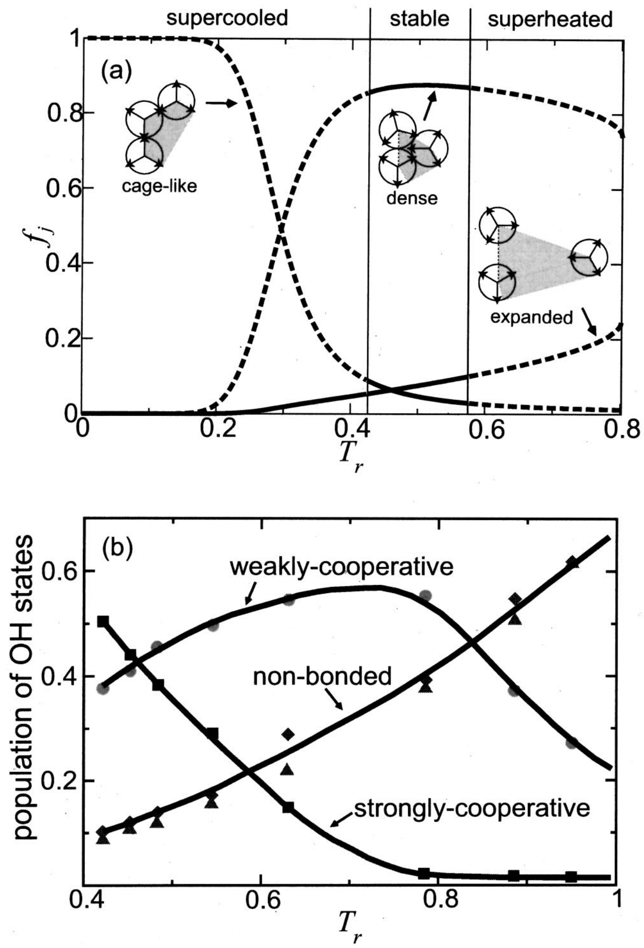

FIG. 3. (a) Triplet populations f_j vs temperature T_r for the model liquid at atmospheric pressure. The vertical lines that bound the stable liquid indicate the freezing and boiling points (see Fig. 4). Parameters are given in Fig. 2. (b) Populations of OH states vs temperature T_r along water's saturation curve as determined from IR spectra (adapted from Fig. 5 of Ref. 3). Curves are guides to the eye.

PHASE DIAGRAM

To study water's phase behavior, we also modeled two crystalline forms: a low-pressure (LP) and a high-pressure (HP) ice. LP ice is an open cagelike solid that has been found in simulations[12] of the MB model at low P and T. The structure of HP ice is identical to that of LP ice, except that there is an additional water molecule in the center of each open cage (see Fig. 4). In other words, HP ice is a self-clathrate.[19] Although these two solids do not exhaust the possible crystals for this model, we have not yet found other stable forms. We treat the model ices via a cell theory approach[16] in which each solid is composed of N identical and independent cells (see Fig. 4). We assume that the solids are incompressible and obtain analytical expressions[14] for the chemical potentials of the two ice forms $\mu_{\mathrm{LP}}(\beta,P)$ and $\mu_{\mathrm{HP}}(\beta,P)$, respectively. Their molar volumes are $v_{\mathrm{LP}} = 3\sqrt{3}d^2/4$ and $v_{\mathrm{HP}} = \sqrt{3}d^2/2$. To compute the various phase boundaries, we set equal the chemical potentials of competing phases [e.g., $\mu(\beta,P) = \mu_{HP}(\beta,P)$ yields the melting curve of HP ice].

Downloaded 15 Mar 2013 to 146.201.208.22. Redistribution subject to AIP license or copyright; see http://jcp.aip.org/about/rights_and_permissions

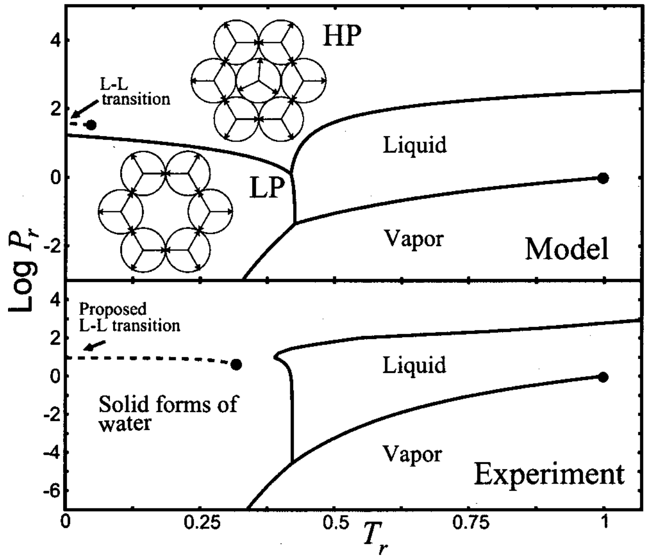

FIG. 4. Phase diagram of the model (top) compared to experiments (bottom) in pressure P_r vs temperature T_r. Unbroken curves are phase boundaries for the transitions discussed in the text. Dashed curves locate the metastable liquid–liquid (L–L) transition in the theory and a schematic of its proposed location in water (see Ref. 8). LP ice consists of open cages in which each molecule bonds to three neighbors. HP ice is identical to LP ice, except that it has an additional molecule in the center of each cage. For clarity, the solid–solid transitions in the experimental phase diagram of water are omitted. Parameters are given in Fig. 2.

Figure 4 shows the model phase diagram for water, compared to experiments. The model predicts a boiling transition that terminates in a critical point, and freezing transitions to LP ice and HP ice at low and high pressure, respectively.[20] In agreement with experiments, LP ice has a negatively sloped melting curve (it contracts upon melting), and HP ice has a positively sloped melting curve (it expands upon melting). The two ice forms are separated by a first-order phase transition. The theoretical melting and boiling curves are shown to converge to a triple point, below which only the vapor or solid states are thermodynamically stable. In agreement with the phase diagram of water, the triple-point temperature is roughly 42% of the vapor–liquid critical temperature.

One additional prediction is interesting. Experiments show that glassy water exhibits an apparent "first-order" transformation between its low-density and high-density forms.[8,21] An insightful conjecture[22] (yet to be experimentally verified[7,8]) is that this transformation reflects an underlying first-order liquid–liquid transition in supercooled water. Consistent with this hypothesis, the present model predicts a low-temperature transition between two supercooled liquid phases. Analysis of the local triplet populations f_j along this coexistence curve reveals that, in analogy with water's experimental glasses,[8,21] the predicted liquid–liquid transition is between an open h-bonded fluid and a densely packed fluid.

CONCLUDING REMARKS

We present an analytical model that describes water as a distribution of three types of microscopic states of molecular triplets: dense and expanded structures (characteristic of simple fluids) and cagelike structures (characteristic of water). It explains many of water's thermodynamic and structural anomalies by the temperature- and pressure-dependent populations of these states. Its qualitative agreement with experiments suggests that accounting for molecular details—long-range electrostatic interactions, polarity, and three-dimensional tetrahedral structure (none of which are treated here)—is less important than treating the balance between localized h-bonding and vdW interactions for capturing pure water's distinctive thermal signatures.

ACKNOWLEDGMENTS

We thank F. H. Stillinger and J. R. Errington for useful discussions. This work was supported by the National Institutes of Health.

1 D. Chandler, J. D. Weeks, and H. C. Andersen, Science **220**, 787 (1983).
2 W. A. P. Luck, in *The Hydrogen Bond*, Vol. 2, edited by P. Schuster, G. Zundel, and C. Sandorfy (Elsevier, Amsterdam, 1976); F. H. Stillinger, Science **209**, 451 (1980); G. A. Jeffrey, *An Introduction to Hydrogen Bonding* (Oxford University Press, New York, 1997); J. D. Cruzan *et al.*, Science **271**, 59 (1996).
3 W. A. P. Luck, J. Mol. Struct. **448**, 131 (1998).
4 F. Weinhold, J. Chem. Phys. **109**, 367 (1998).
5 F. Weinhold, J. Chem. Phys. **109**, 373 (1998).
6 C. A. Angell, Annu. Rev. Phys. Chem. **34**, 593 (1983).
7 P. G. Debenedetti, *Metastable Liquids* (Princeton University Press, Princeton, 1996).
8 O. Mishima and H. E. Stanley, Nature (London) **396**, 329 (1998).
9 P. H. Poole, F. Sciortino, T. Grande, H. E. Stanley, and C. A. Angell, Phys. Rev. Lett. **73**, 1632 (1994).
10 T. M. Truskett, P. G. Debenedetti, S. Sastry, and S. Torquato, J. Chem. Phys. **111**, 2647 (1999).
11 A. Ben-Naim, J. Chem. Phys. **52**, 3682 (1971).
12 K. A. T. Silverstein, A. D. J. Haymet, and K. A. Dill, J. Am. Chem. Soc. **120**, 3166 (1998).
13 We prefer the term "volume" here to maintain consistency with the 3D systems we are modeling. In this 2D model, these quantities are areas.
14 T. M. Truskett and K. A. Dill (unpublished).
15 E. A. Jagla, J. Chem. Phys. **111**, 8980 (1999).
16 T. L. Hill, *Statistical Mechanics: Principles and Selected Applications* (Dover, New York, 1956).
17 References 14 and 15 discuss how to account for the dispersion attractions when computing the model's thermodynamic properties.
18 G. S. Kell, J. Chem. Eng. Data **12**, 66 (1967); R. J. Speedy and C. A. Angell, J. Chem. Phys. **65**, 851 (1976); C. A. Angell, M. Oguni, and W. J. Sichina, J. Phys. Chem. **86**, 998 (1982); D. E. Hare and C. M. Sorensen, J. Chem. Phys. **84**, 5085 (1986).
19 L. Pauling, *The Nature of the Chemical Bond* (Oxford University Press, London, 1939).
20 The present theory neglects crystal defects and predicts first-order melting transitions. Note that Kosterlitz–Thouless–Halperin–Nelson–Young theory predicts that defects can cause the melting of 2D crystals to occur via a continuous transition [see, e.g., K. J. Strandburg, Rev. Mod. Phys. **60**, 161 (1988)].
21 O. Mishima, L. D. Calvert, and E. Whalley, Nature (London) **314**, 76 (1985).
22 P. H. Poole, F. Sciortino, U. Essman, and H. E. Stanley, Nature (London) **360**, 324 (1992).

Downloaded 15 Mar 2013 to 146.201.208.22. Redistribution subject to AIP license or copyright; see http://jcp.aip.org/about/rights_and_permissions